

# $k$ spectra of Thomson scattering temperature profiles at the TJ-II stellarator

B.P. van Milligen, I. Pastor, J. Herranz, F. Castejón  
Laboratorio Nacional de Fusión por Confinamiento Magnético,  
Asociación Euratom-CIEMAT,  
Madrid, Spain

**Abstract.** High resolution Thomson scattering temperature profiles at the TJ-II stellarator are subjected to spectral analysis. The obtained  $k$  spectrum is very robust in shape. While its amplitude has been shown previously to scale inversely with the collisionality, here it is found that its shape is independent of plasma configuration (magnetic well, iota), global plasma parameters (temperature, density) and radial position (centre, edge). The shape is also found to be very similar to that of  $k$  spectra obtained with Langmuir probes in the edge of TJ-II and of  $k$  spectra obtained using other techniques in other devices. The spectral shape is characterized by a ‘knee’ at  $k = 500\text{--}1000\text{ m}^{-1}$  and a steep decay at large  $k$ . Self-similarity analysis reveals the existence of a high degree of self-organization dominated by structures of around 2.5 cm in size.

## 1. Introduction

Over recent years, an interesting series of papers has appeared describing the observation of structures in measured Thomson scattering temperature and density profiles [1–3]. These structures are local peaks or valleys of considerable amplitude and having a radial extent of about 1 cm. They are particularly prominent in regions where the local heating density, produced by the ECRH power injection, is high, and decay in amplitude when the ECRH is switched off [2].

Several mechanisms have been put forward to explain the appearance of these structures. The structures might be related to the existence of magnetic islands (either ‘natural’ — in a stellarator only — or induced by the current distribution within the plasma) having a different heat or particle confinement than the ambient plasma, leading to strongly different temperatures or densities within the islands, especially when a local heating method is applied (i.e. ECRH). On the other hand, kinetic effects induced by ECRH might play a role. A possible explanation for the structures based on plasma ‘filaments’, i.e. local current concentrations, was put forward at RTP [1, 2]. Finally, broadband turbulence might be involved.

A comparison between profiles of the Thomson scattering diagnostics of the RTP and TJ-II fusion devices would be very interesting, because the two diagnostic systems have similar spatial resolution and observe plasmas of similar size, while the magnetic configuration is quite different: RTP is a

tokamak with high shear and many low order rational surfaces, while TJ-II is a low shear heliac with few low order rational surfaces. Such a comparison might shed some light on the nature of the structures (in particular their association with magnetic topology).

However, it has in general been very difficult to associate the observed structures with the magnetic topology owing to a lack of precise experimental information on the latter (i.e. lack of knowledge of the internal plasma current distribution). Further, the structures mostly do not exhibit the regular behaviour (symmetric or anti-symmetric with respect to the magnetic axis) that is expected for phenomena associated with magnetic islands, with a few exceptions. For clarity we stress that the structures we discuss in this article are not taken to include the steep slopes that were observed and convincingly shown to be associated with transport barriers close to rational surfaces at RTP, but only local peaks or valleys.

In this article, we explore a new route of analysis and study the  $k$  spectrum of the observed fluctuations. The spectrum provides information on the distribution function of the structure size, and we try to link that distribution function to a possible explanation.

## 2. Experimental set-up

Figure 1 shows the high resolution, multiposition Thomson scattering system, which routinely

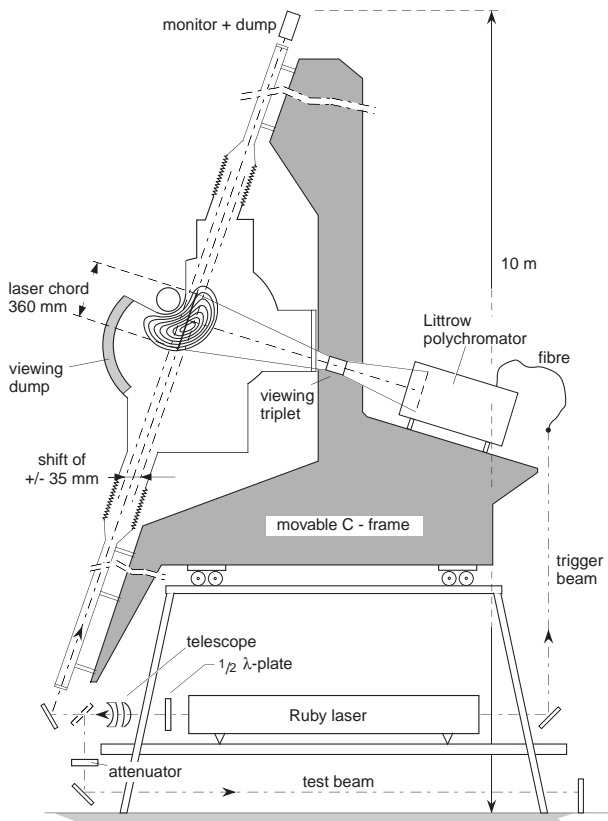


**Figure 1.** Layout of the Thomson scattering system at TJ-II.

measures electron temperature and density profiles in the TJ-II stellarator ( $R = 1.5$  m,  $a < 0.22$  m,  $B_0 < 1$  T) [4]. The system can measure electron temperatures in the range 50 eV to 4 keV. The resolution of the system amounts to three CCD image pixels ( $22 \mu\text{m}$  each) in the  $z$  direction and four pixels in the wavelength direction. As a result the spatial resolution is 2.25 mm and the spectral resolution is 2.4 nm, giving 160 spatial and 90 spectral elements [5]. With this spatial resolution, the system is among the few able to resolve small scale structures in the density and temperature profiles. The spectrometer and laser branch are mounted on a 9 m high movable structure, which allows a maximum radial excursion of the laser chord by 70 mm, enabling it to follow the position of the magnetic axis of the different TJ-II magnetic configurations. Currently only a single profile per shot can be obtained, owing to the limitation of the laser energy to 10 J per pulse.

Further details of the Thomson scattering system can be found in Ref. [5].

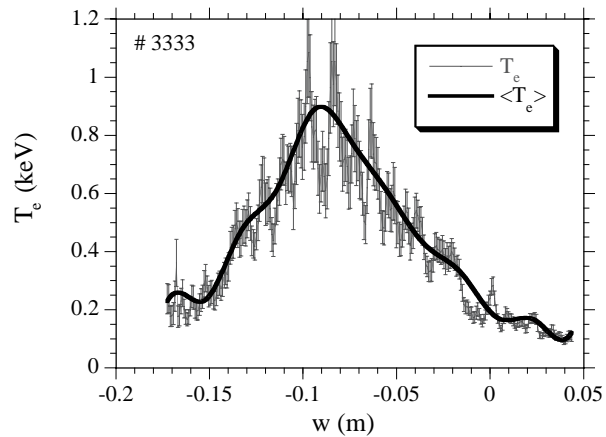


**Figure 2.** Thomson profile with error bars and spline fit (10 knots).

### 3. Spectral analysis

The analysis of the Thomson profiles is done using standard analysis methods. The profile consists of about 280 useful data values, equally spaced along an observation chord traversing the plasma. The co-ordinate along the chord is denoted by  $w$  (m). This co-ordinate is a real space co-ordinate and can be converted to flux co-ordinates using a mapping corresponding to a flux surface geometry, calculated theoretically from the experimental currents in the main coils. However, owing to the uncertainties in this mapping we prefer to use the real space co-ordinate  $w$  and will do so throughout this article.

A spline curve with between 10 and 20 knots is fitted to the profile  $T_e(w)$ . This smooth fit is denoted by  $\langle T_e \rangle$  (Fig. 2). The normalized difference profile,  $(T_e - \langle T_e \rangle) / \langle T_e \rangle$ , is subjected to further analysis. The reason for using this normalization lies in the fact that at TJ-II the fluctuations in the Thomson  $T_e$  profile,  $\Delta T_e$ , are generally proportional to the temperature  $T_e$  itself ( $\Delta T_e \propto T_e$ ), so that the normalization roughly equalizes the weight of the central and edge fluctuations in the subsequent analyses (Fig. 3). Evidently the higher the number of knots used in the spline fit, the more structure is removed from the difference profile. However, by limiting the number of knots to a maximum of 20, structures smaller than a few centimetres ( $k \geq 300 \text{ m}^{-1}$ ) are not affected.

To investigate the contribution of the various fluctuation scale lengths to the profile, the normalized profile is subjected to the wavelet transform (using the Morlet wavelet). Similar results to the ones presented in the following may also be obtained using the Fourier transform, but the precision afforded by the wavelet transform is far superior owing to the

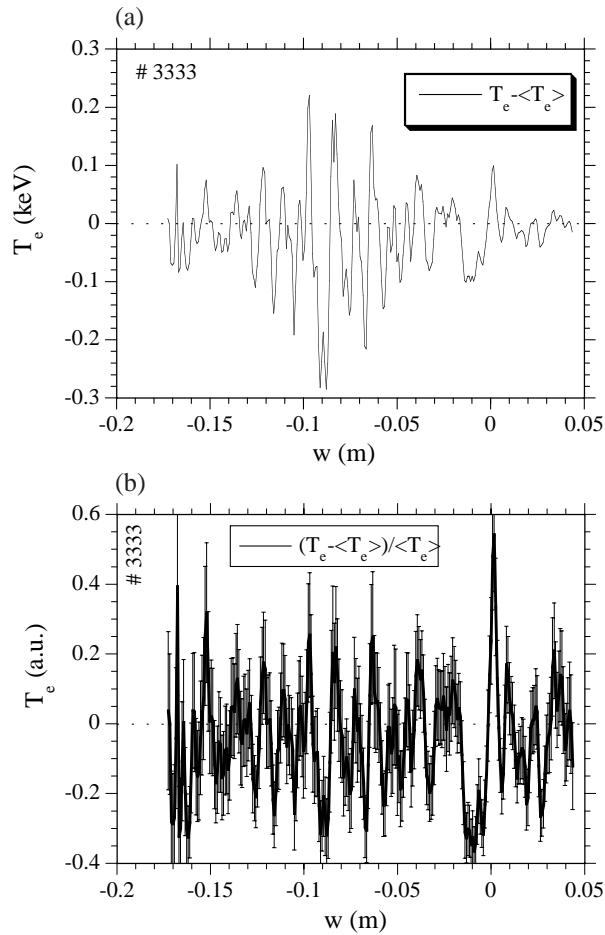


**Figure 3.** (a) Difference Thomson profile; (b) normalized difference Thomson profile and error bars.

comparatively short length of the data record (around 280 points per discharge). Also, the wavelet transform does not average the spatial information so that structures of different size may be related to their position in the plasma. A typical wavelet transform of a profile is shown in Fig. 4. Contributions of the small and large scale lengths are separated according to their  $k$  value (wavenumber) and position. It is immediately clear that any differences between the edge and central plasma regions are small.

To obtain an average  $k$  spectrum for every discharge, the wavelet spectra are integrated along the  $w$  co-ordinate. The results of such an averaging process are shown in Fig. 5. Here the wavelet spectra from 20 discharges obtained in one day of operation are averaged. The calculation was done both for the original  $T_e$  profile and the normalized  $T_e$  profile. The spectrum is characterized by: (1) the existence of a ‘knee’ in the spectrum at around  $500$ – $1000$   $\text{m}^{-1}$ , and (2) the decay of the spectra at high

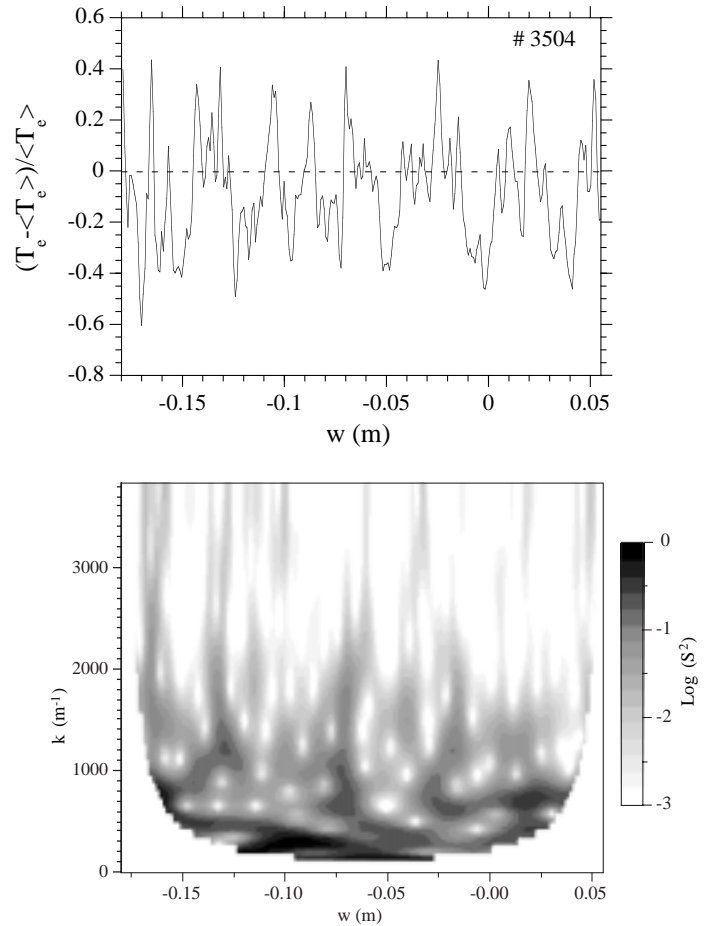


**Figure 4.** A normalized Thomson profile (top panel) and its corresponding wavelet transform (bottom panel).

$k$  values. Note that the ‘hump’ seen in Fig. 5 for  $3000 < k < 4000$   $\text{m}^{-1}$  is caused by the analysis technique used and is not significant. In the remaining graphs, this part of the spectrum is omitted. Finally, the optical resolution of the Thomson scattering diagnostic is  $2.25$   $\text{mm}$ , corresponding to a wavenumber of  $k = 1400$   $\text{m}^{-1}$ . Larger values of  $k$  cannot be resolved by the diagnostic. Altogether, the spectra presented here are only significant for values of  $k$  in the range  $300 < k < 1400$   $\text{m}^{-1}$ .

### 3.1. Error analysis

An important aspect of any study of Thomson scattering profiles is its error analysis. As described in more detail in Ref. [3] and references therein, a thorough analysis of possible errors contributing to the measured temperature and density profiles has been performed. This analysis takes into account the contributions of photon noise in the first image intensifier due to light from the scattering volume

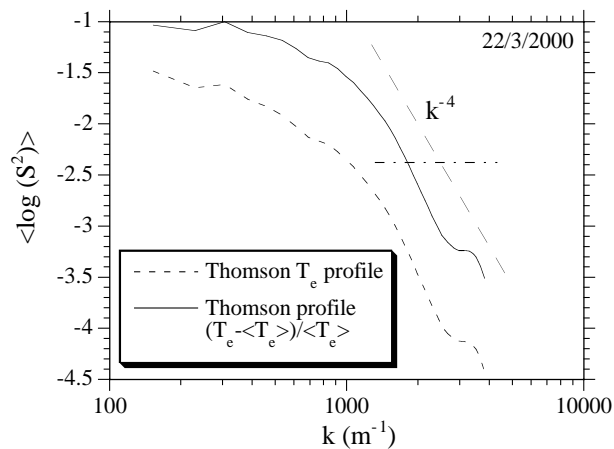


**Figure 5.** Average wavelet spectra of one day of operation (average over 20 discharges). The dashed–dotted horizontal line is the error level corresponding to the spectrum of the normalized profiles only, for  $N = 20$  (see Section 3.1).

in the plasma, and the instrumental function of the optical and electronic detection system, as well as the errors due to the numerical processing needed to extract temperatures and densities from the measured scattering spectra. It results in an error bar for each measured point in the profile. In Fig. 2, these error bars are drawn. It is clear that the amplitude of some structures exceeds the size of the error bars.

To estimate the effect of these errors on the  $k$  spectrum, an error simulation was performed. First, 34 discharges from a typical measurement session of one day were taken. In this carefully selected series of shots, the plasma conditions were held as constant as possible. For each discharge, a profile and the corresponding error bars were obtained. The information on the 34 discharges (profiles and error bars) was then averaged. The average temperature profiles still showed some roughness, which was removed using a 30 point cosine bell smoothing filter. This averaged, smoothed and structureless profile was used as a starting point for a Monte Carlo simulation in which the profile was modified by adding Gaussian noise to each profile point. The width of the Gaussian noise distribution at each point was taken equal to the error bar at that point. For each resulting profile, a spectrum was computed in the manner described above. This process was repeated 50 times, and the resulting spectra were averaged. Thus an average noise spectrum was obtained. This noise level spectrum is accurately represented by the straight line  $\langle \log S^2(k) \rangle = -1.73$ . Note that all logarithms are base 10 in this article.

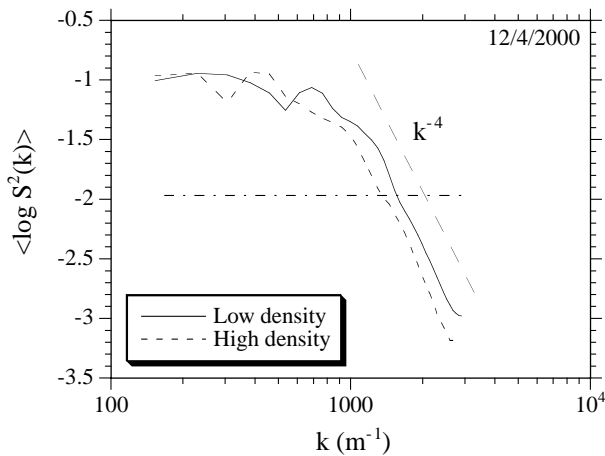


**Figure 6.** Average wavelet spectra as a function of density. Low density: five discharges, high density: three discharges. The error level corresponding to  $N = 3$  (see Section 3.1) is indicated by the dashed–dotted horizontal line.

Because this noise source, dominated by the photon noise, is statistically independent from discharge to discharge, the noise level may be reduced by averaging measurements from different discharges. So when  $N$  spectra are averaged, the noise level is reduced to the level  $-1.73 - (\log N)/2$ . This line is indicated in all plots of spectra, thus highlighting the part of the spectrum that is above noise level.

### 3.2. Amplitude of the $k$ spectrum

The amplitude of the obtained  $k$  spectrum (i.e. the root mean square (RMS) value of the profile) is found to depend in a rather predictable way on global plasma parameters. In a previous publication, the RMS value of the oscillations of the profile was found to scale with  $T_e^{3/2}/n$ , i.e. approximately inversely with the electron–ion collision frequency, with a correlation coefficient of  $R = 0.85$  [3]. So as the electron density  $n_e$  is increased, the RMS value of the oscillations of the profile is reduced (Fig. 6). This basic dependence may explain the following two observations: (a) When the heating power is increased, the RMS value is reduced (Fig. 7) owing to the fact that power and density are coupled in the TJ-II stellarator (in other words, an increase in the power delivered by the gyrotrons tends to increase mainly the density, without having a pronounced effect on the temperature). (b) When the depth of the magnetic well is increased (leading to increased stability), the RMS value is also reduced (Fig. 8).

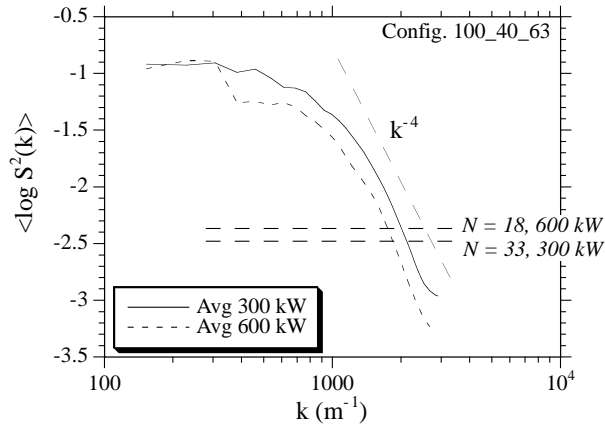


**Figure 7.** Spectrum as a function of heating power. Average over 33 discharges (300 kW) and 18 discharges (600 kW). The horizontal dashed lines indicate the error level corresponding to each case (see Section 3.1).

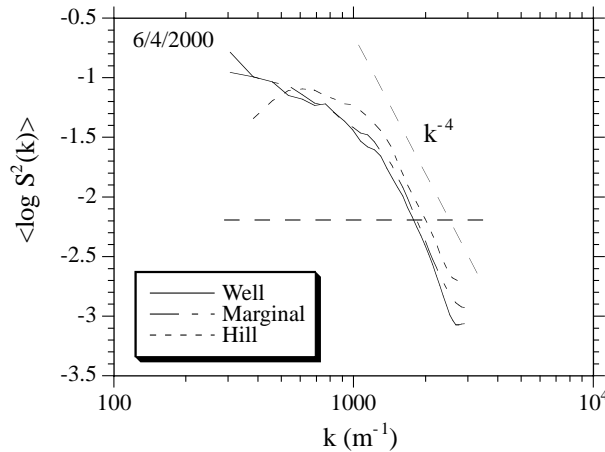


**Figure 8.** Spectrum as a function of magnetic well. Average over 4 discharges (Well: well = 2.4%), 9 discharges (Marginal: well = 0.95%) and 12 discharges (Hill: well = 0.2%). The horizontal dashed line indicates the error level corresponding to the case  $N = 9$  (see Section 3.1).

### 3.3. Shape of the $k$ spectrum

We have studied the dependence of the shape of the  $k$  spectrum on several parameters. First, we investigated whether the spectrum depends on the radial position. The Thomson profiles have sufficient points to split the profiles into a central and an edge region. Owing to the need for a minimum amount of data for calculating the spectrum, no further radial subdivisions can be made. Figure 9 shows the  $k$  spectra for both regions. No significant difference in the spectra is observed at large  $k$ .

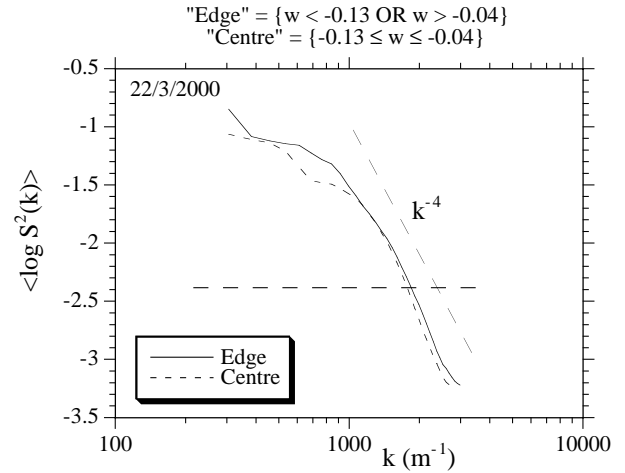


**Figure 9.** Spectra from the edge and the centre (averaged over 20 discharges). The horizontal dashed line indicates the error level (see Section 3.1).

Secondly, we studied whether the spectra depend on the plasma configuration. To do so, we have investigated discharges with configurations having different values of the magnetic well, i.e. 2.4% ('well' case), 0.95% ('marginal' case) and 0.2% ('hill' case) (Fig. 8), and iota (not shown). The configurations with low average well have a magnetic hill at the plasma edge. Although these configurations do not exhaust the complete range of possible TJ-II configurations available through its configurational flexibility, it is interesting to note that no significant change in shape is observed for the cases mentioned above.

Thirdly, we have studied the dependence of the shape of the  $k$  spectra on electron density and heating power while keeping the magnetic configuration fixed (Figs 6 and 7). Again, no significant dependence of the spectral shape was observed (but note the dependence of the spectral amplitude mentioned previously).

### 3.4. Comparison with other techniques and other devices

In Fig. 10, some typical  $k$  spectra obtained with triple Langmuir probes [6] in the plasma edge are shown. The  $k$  values are calculated from measurements of the floating potential made simultaneously by two probe tips which are separated poloidally by 2.5 mm. The calculation of the  $k$  spectra is done using the standard method described in Ref. [7]. The obtained  $k$  spectra of the (propagating) edge fluctuations show the same characteristics (position of the

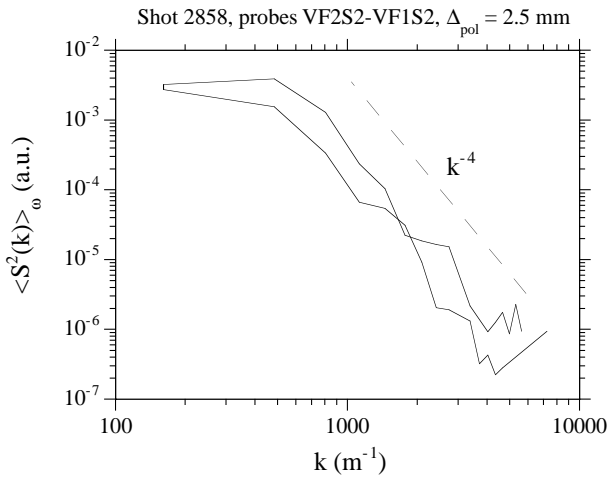


**Figure 10.**  $k$  spectra from probe data (a single discharge).

knee, decay at large  $k$ ) as the Thomson scattering profile  $k$  spectra.

Such spectra are typical for turbulence in fusion devices and have also been observed in other devices. In Ref. [8], a radial  $k$  spectrum of  $n_e$  fluctuations in the plasma core is reported that has a clear knee at about  $100 \text{ m}^{-1}$  shown by beam emission spectroscopy measurements at the TFTR tokamak. In Ref. [9], a turbulent  $k$  spectrum of  $n_e$  fluctuations in the plasma edge is observed that has a knee at around  $200 \text{ m}^{-1}$  shown by probe measurements at the ADITYA tokamak. Here the decay index  $\alpha$  of the power spectrum  $S^2(k) \propto k^{-\alpha}$  at large  $k$  is about 4. In Ref. [10], the  $k$  spectrum of  $n_e$  fluctuations is reported for turbulence in the edge region of the TEXT tokamak as measured by both Langmuir probes and FIR scattering. Good agreement between the two measurements is found, and the radial  $k$  spectrum shows a knee at about  $200\text{--}400 \text{ m}^{-1}$  and has a decay index for large  $k$  of about 4. Finally, in Ref. [11], again at the TEXT tokamak, power spectra are reported for measurements of  $n_e$  fluctuations made with the heavy ion beam probe diagnostic at a radial position of about  $r/a = 0.6$ . From the information given, it may be deduced that the spectrum also possesses a knee, located roughly at  $k = 100 \text{ m}^{-1}$ .

### 3.5. Self-similarity analysis

The Thomson scattering profiles are short records ( $<300$  points) that do not allow detailed fractal analyses. At best, one may investigate the self-similarity of the profiles to some extent. For this purpose, we

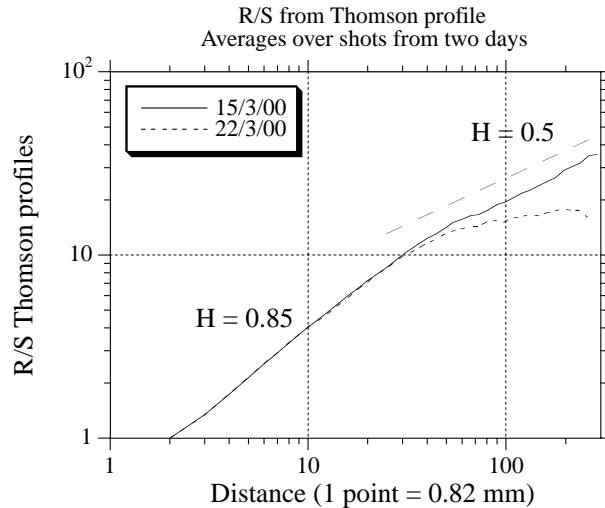


**Figure 11.**  $R/S$  analysis of Thomson profiles, averaged over 34 discharges (15/3/00) and 20 discharges (22/3/00).

have applied the Hurst analysis to the profiles [12]. Results are shown in Fig. 11. The  $R/S$  graph always displays a steep logarithmic slope ( $H = 0.85$ ) for distances of less than about  $2.5 \text{ cm}$ . This straight slope is indicative for self-similarity for scales smaller than this cut-off size, suggesting that the corresponding structures are not random but self-organize in a structured pattern. For large distances ( $>2.5 \text{ cm}$ ), the correlation is lost or becomes negative, depending on the case. One may speculate that this long range behaviour is associated with the magnetic topology. However, it is not clear whether the Hurst parameter for large distances shows any dependence on global parameters.

## 4. Discussion and conclusions

The power spectrum of the Thomson scattering temperature profile shows a knee at  $k = 500\text{--}1000 \text{ m}^{-1}$  and decays at large  $k$  (Fig. 12). The value of the decay exponent cannot be determined with precision owing to the fact that the significance of the spectra is limited by the spatial resolution at  $k = 1400 \text{ m}^{-1}$ , although it seems to be compatible with the typical  $k^{-4}$  decay seen also by other diagnostics. The characteristics of the  $k$  spectrum of the Thomson scattering electron density profile are very similar to the reported results for the temperature profile. The position of the knee does not seem to bear any relation to the ion Larmor radius  $\rho_s$ , which varies from about  $0.5 \text{ mm}$  at the plasma edge to about  $4 \text{ mm}$  in the plasma centre. It may,

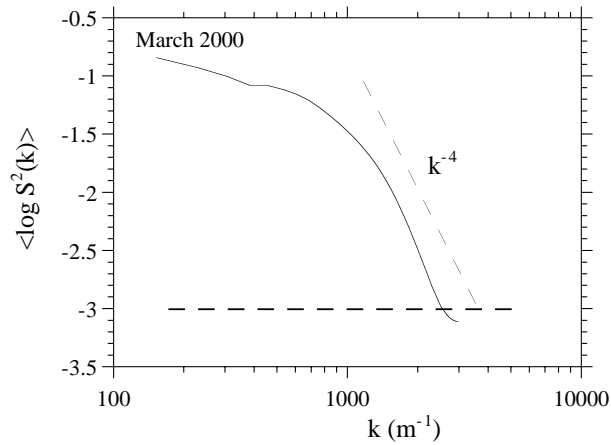


**Figure 12.** Average  $k$  spectrum of 359 discharges. The horizontal dashed line indicates the error level (see Section 3.1).

however, be related to the radial turbulence correlation length  $\lambda_r$ , which is of the order of 1 cm or less. The shape of the  $k$  spectrum is not very sensitive to the particular plasma configuration or global plasma parameters and does not vary significantly from the plasma centre to the plasma edge. Moreover, the shape is very similar to that of the  $k$  spectra obtained from Langmuir probes in the edge and measurements of  $k$  spectra made in other fusion devices, the characteristics of the spectra (position of the knee and value of the decay exponent) being roughly of the same order for all devices. At TJ-II, the RMS value of the profile fluctuations (i.e. the amplitude of the spectrum) varies in a predictable way with the global plasma parameters (through the collisionality).

As mentioned in the introduction, there exist various hypotheses as to the nature of these fluctuations, of which we cite four: (a) magnetic islands (natural or otherwise), (b) kinetic effects related to ECRH, (c) filaments and (d) broadband turbulence. The observations are (1) that the amplitude of the oscillations scales roughly with the inverse of the collision frequency, and (2.1) that the shape of the  $k$  spectrum is robust and (2.2) very similar to the turbulent spectrum measured with other techniques

and in other devices. Observation (1) suggests that hypothesis (b), kinetic effects, may be of importance as a driving term. Observations (2.1, 2.2) seem to favour an explanation in terms of hypothesis (d), broadband turbulence. The fact that no particular structure (peaks) is detected in the  $k$  spectrum also suggests that broadband turbulence may be more important than, for example, topological effects. It is not clear what kind of  $k$  spectrum hypothesis (c), filaments, would produce. Nevertheless, there are also many convincing arguments in favour of a link with the underlying magnetic topology (cf. the RTP experiments; however, recall that the underlying magnetic topology is fundamentally different for a tokamak). Perhaps a combination of several effects is needed to reach a complete and satisfactory understanding of the observed structures.

## References

- [1] Lopes Cardozo, N.J., et al., Phys. Rev. Lett. **73** (1994) 256.
- [2] Lopes Cardozo, N.J., et al., Plasma Phys. Control. Fusion **39** (1997) B303.
- [3] Herranz, J., et al., Phys. Rev. Lett. **85** (2000) 22.
- [4] Alejandre, C., et al., Plasma Phys. Control. Fusion **41** (1999) A539.
- [5] Barth, C.J., et al., Rev. Sci. Instrum. **70** (1999) 763.
- [6] Pedrosa, M.A., et al., Rev. Sci. Instrum. **70** (1999) 415.
- [7] Beall, J.M., Kim, Y.C., Powers, E.J., J. Appl. Phys. **53** (1982) 3933.
- [8] Fonck, R.J., et al., Phys. Rev. Lett. **70** (1993) 3736.
- [9] Jha, R., Kaw, P.K., Phys. Rev. Lett. **69** (1992) 1375.
- [10] Ritz, C.P., et al., Nucl. Fusion **27** (1987) 1125.
- [11] Ross, D.W., et al., Nucl. Fusion **31** (1991) 1355.
- [12] Carreras, B.A., et al., Phys. Plasmas **5** (1998) 3632.

(Manuscript received 18 September 2000)

Final manuscript accepted 18 January 2001)

E-mail address of B.P. van Milligen:  
boudewijn.vanmilligen@CIEMAT.es

Subject classification: D2, Se; K0, Se